NASA TECHNICAL NOTE

NASA TN D-2880

APOLLO ENTRY TRACKING: A SHIPBOARD UNIFIED S-BAND INTERFEROMETER SYSTEM

by F. O. Vonbun

Goddard Space Flight Center
Greenbelt, Md.

NATIONAL AERONAUTICS AND SPACE ADMINISTRATION • WASHINGTON, D. C. • AUGUST 1965

NASA TN D-2880

APOLLO ENTRY TRACKING:

A SHIPBOARD UNIFIED S-BAND

INTERFEROMETER SYSTEM

By F. O. Vonbun

Goddard Space Flight Center
Greenbelt, Md.

NATIONAL AERONAUTICS AND SPACE ADMINISTRATION

For sale by the Clearinghouse for Federal Scientific and Technical Information
Springfield, Virginia 22151 – Price $2.00

APOLLO ENTRY TRACKING: A SHIPBOARD UNIFIED S-BAND INTERFEROMETER SYSTEM

by
F. O. Vonbun
Goddard Space Flight Center

SUMMARY

An outline of the re-entry tracking and communication problem, including a possible solution, is presented in this paper. The acquisition of the lifting Apollo spacecraft after it enters the earth's atmosphere is a difficult problem for tracking which requires particular attention. An interferometer especially developed for this purpose is described and the major design parameters are given. A re-entry network configuration is presented, and the necessary tracking tasks outlined. Blackout problems, re-entry trajectory ground tracking errors and the best ship positioning are discussed in detail.

CONTENTS

Summary iii

INTRODUCTION. 1

APOLLO RE-ENTRY TRAJECTORIES 5

PROBLEMS OF SPACECRAFT ACQUISITION 7

SPECIAL RE-ENTRY ACQUISITION SYSTEMS 9

TRACKING-STATION LOCATIONS ALONG THE RE-ENTRY GROUND TRACK 12

- Communications Blackouts 16
- Tracking Acquisition Angle 16
- Spacecraft Position and Velocity Errors 16
- Ship Prepositioning 18

CONCLUSION 20

ACKNOWLEDGMENTS 21

References 21

Appendix A—List of Symbols Used 23

APOLLO ENTRY TRACKING: A SHIPBOARD UNIFIED S-BAND INTERFEROMETER SYSTEM*

by
F. O. Vonbun
Goddard Space Flight Center

INTRODUCTION

This report has two purposes: to analyze ground tracking and communications problems associated with manned re-entry vehicles, and to develop practical ways and means to solve these problems. An Apollo-type lifting vehicle is considered as the entering spacecraft; its approach to earth is at nearly parabolic speed and with a shallow entry angle. A nominal skip trajectory of approximately 5000 nautical miles (Reference 1) with a lift-to-drag ratio of 0.5 and an entry angle of -6.4° is used for an example.

In a real mission, to be effective, ground support must be almost independent of the particular trajectory chosen; thus, a nominal straight-line ground track (as shown in Figures 1, 2, and 3) cannot be assumed. The ground system must be capable of covering all possible lifting trajectories that the spacecraft could fly after it enters the earth's atmosphere. The only assumption that is made here is that the first re-entry point (point #1 in Figures 1 through 5) is known to be within twenty nautical miles of that planned a few hours before actual re-entry. This is necessary because a re-entry ship cannot move to position fast enough to assure coverage of the skipout portion indicated in the figures mentioned above. This is not a major restriction, however, since it will be shown that the re-entry point can be determined well within the allowable limits from early return-trajectory measurements made by use of the large-dish (85') facilities of the Apollo network.

No other restrictions are treated, but since the spacecraft can fly any trajectory within its capability after its first re-entry, and since the ground system must acquire it without benefit of information as to its present location, the hemispherical acquisition capability of the ground tracking system is considered. It is shown that an interferometer has this capability and is, therefore, employed as spacecraft acquisition system.

Blackout areas occurring along the re-entry track due to the transfer of spacecraft kinetic energy into heat demand attention. These areas are important in the choice of position for the

*Originally published as Goddard Space Flight Center Document X-513-64-85, March 6, 1964.

re-entry ship along the track so that tracking and communication with the spacecraft during the early phase of the skipout may proceed as planned. Investigation of the blackout phenomenon is underway at present,* and it is anticipated that the outcome of this effort will yield a more thorough understanding of this phenomenon and thus make possible better predictions of the blackout areas (see Figures 1, 3, and 5), while also giving insight as to methods for combating the blackout problem itself.

Only the re-entry phase of the spacecraft is discussed. The re-entry phase is assumed to be that portion of the flight starting with the first buildup of dynamic pressure (≐ 0.05g, occurring at approximately 400,000 feet for an Apollo-type spacecraft, see Figure 1) to the opening of the drag chute (≐ 90,000 to 70,000 feet). At present, Goddard Space Flight Center is developing a re-entry interferometer system. The system incorporates a 1.5-meter crossed baseline utilizing five antennas; it will have an electrical phase error on the order of one degree and an angle error of 0.5 to 3 milliradians over an elevation angle variation of 90° to 10°.

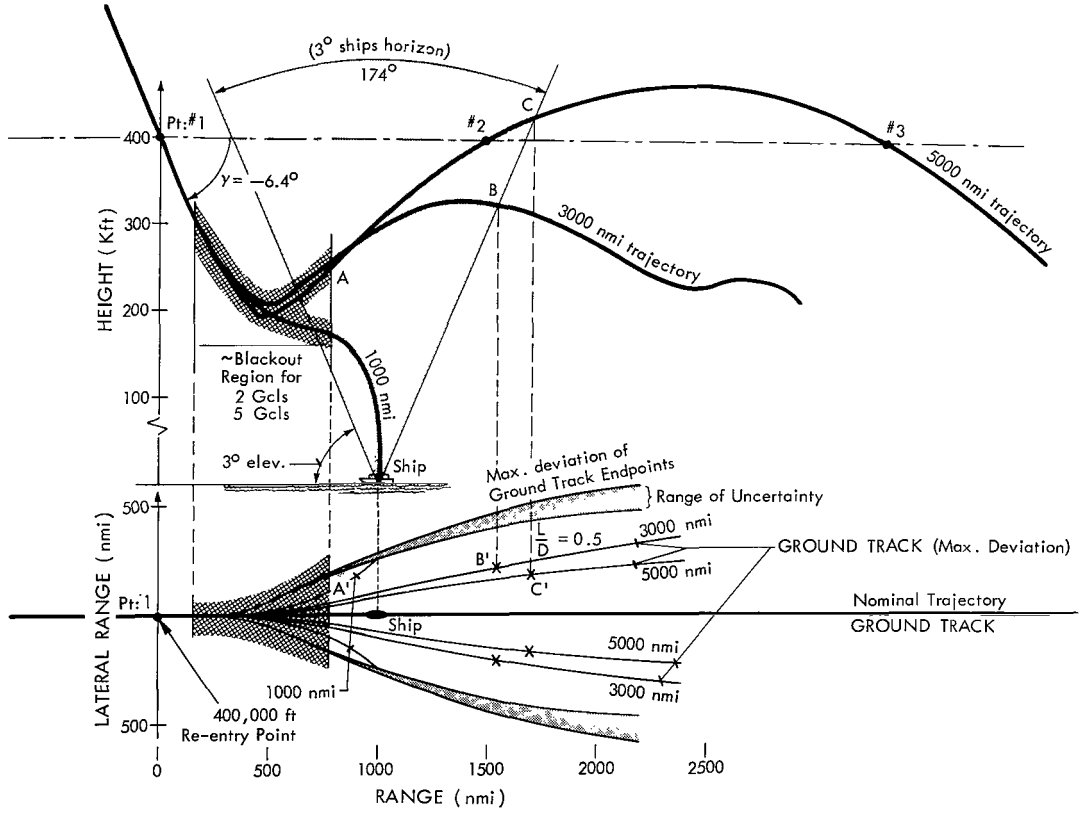

Figure 1—Apollo re-entry trajectories (horizontal and vertical projections).

*This investigation is being conducted by both the Goddard Space Flight Center and the Cornell Aeronautical Laboratory.

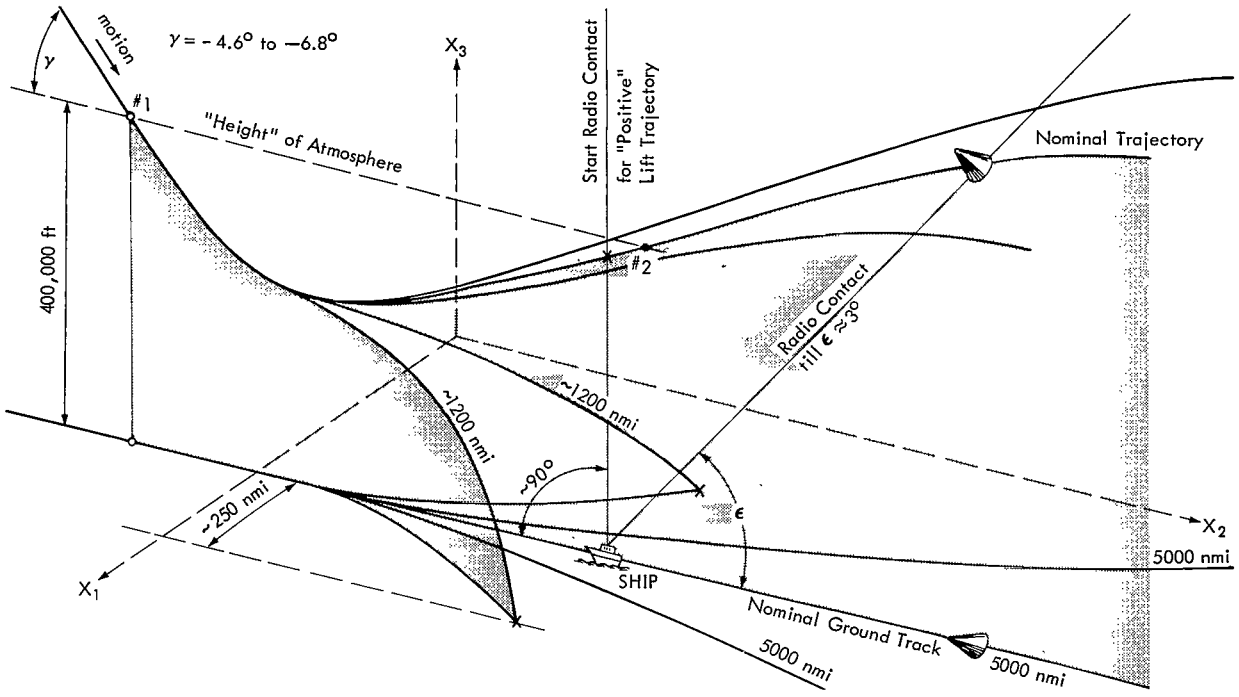

Figure 2—Re-entry trajectories in three dimensions.

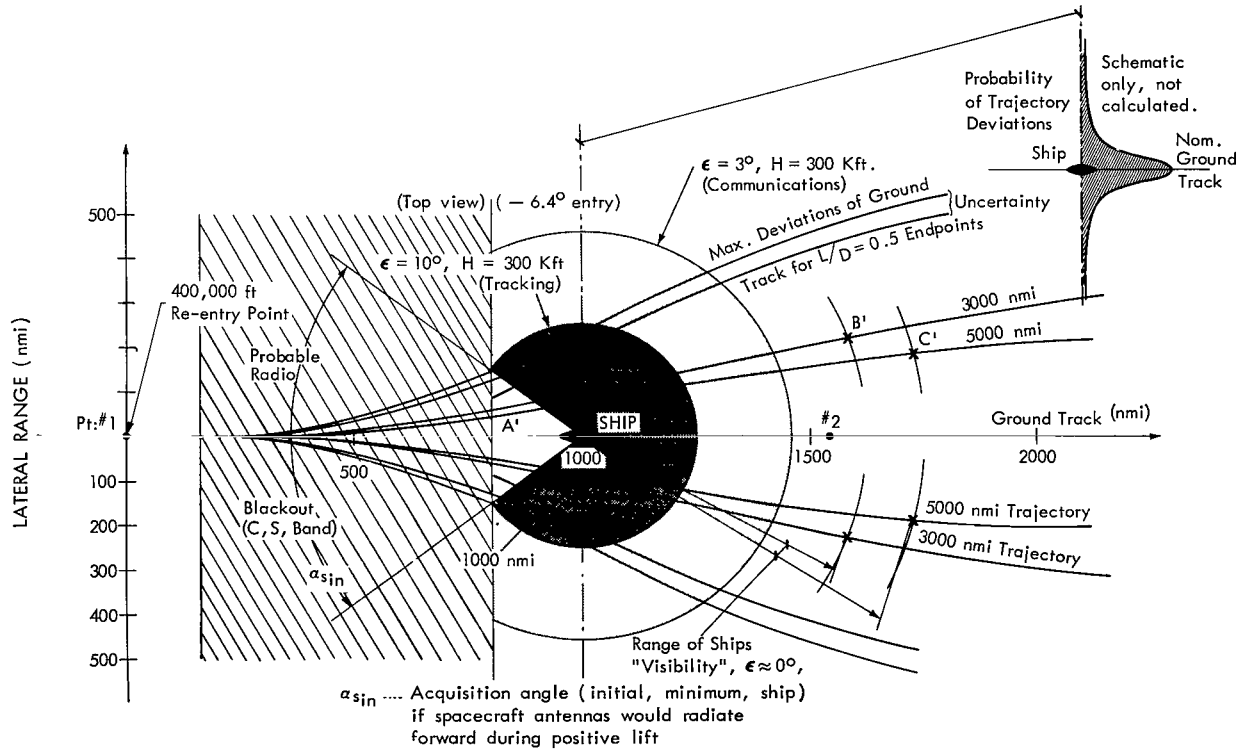

Figure 3—Apollo re-entry ground tracks.

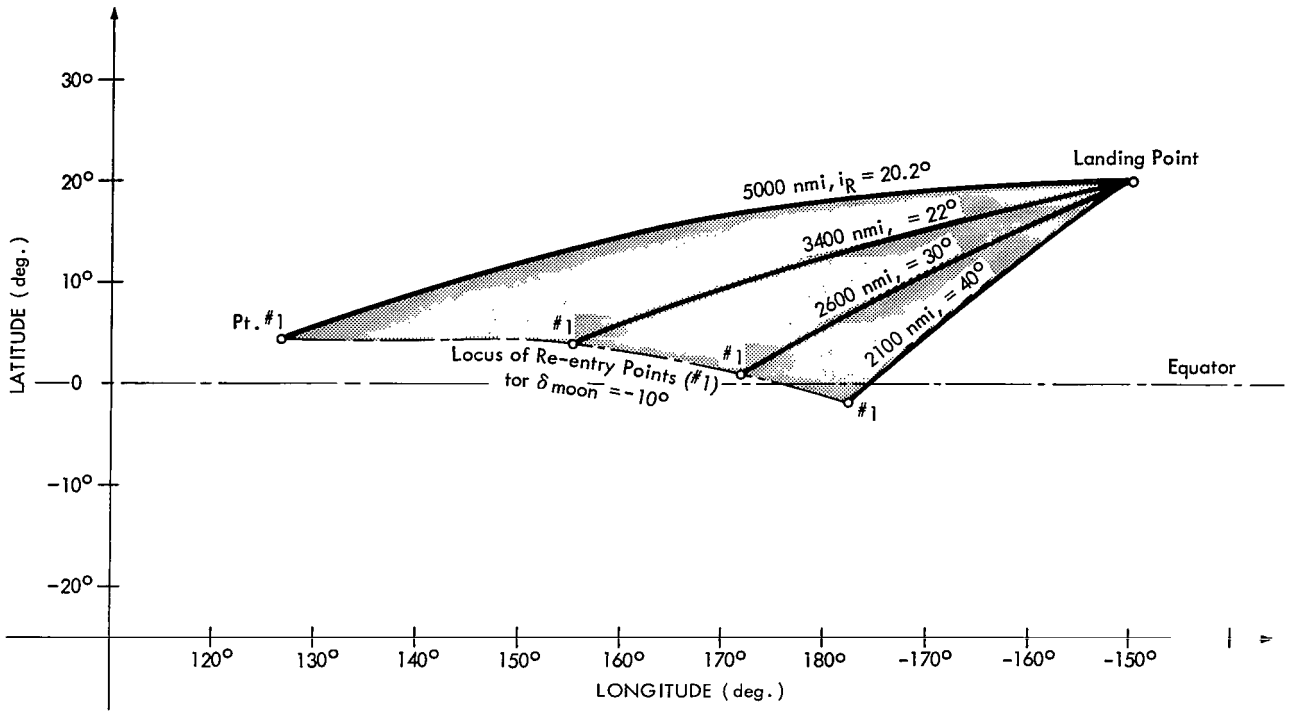

Figure 4—Re-entry ground tracks for various lunar return inclinations, i_R.

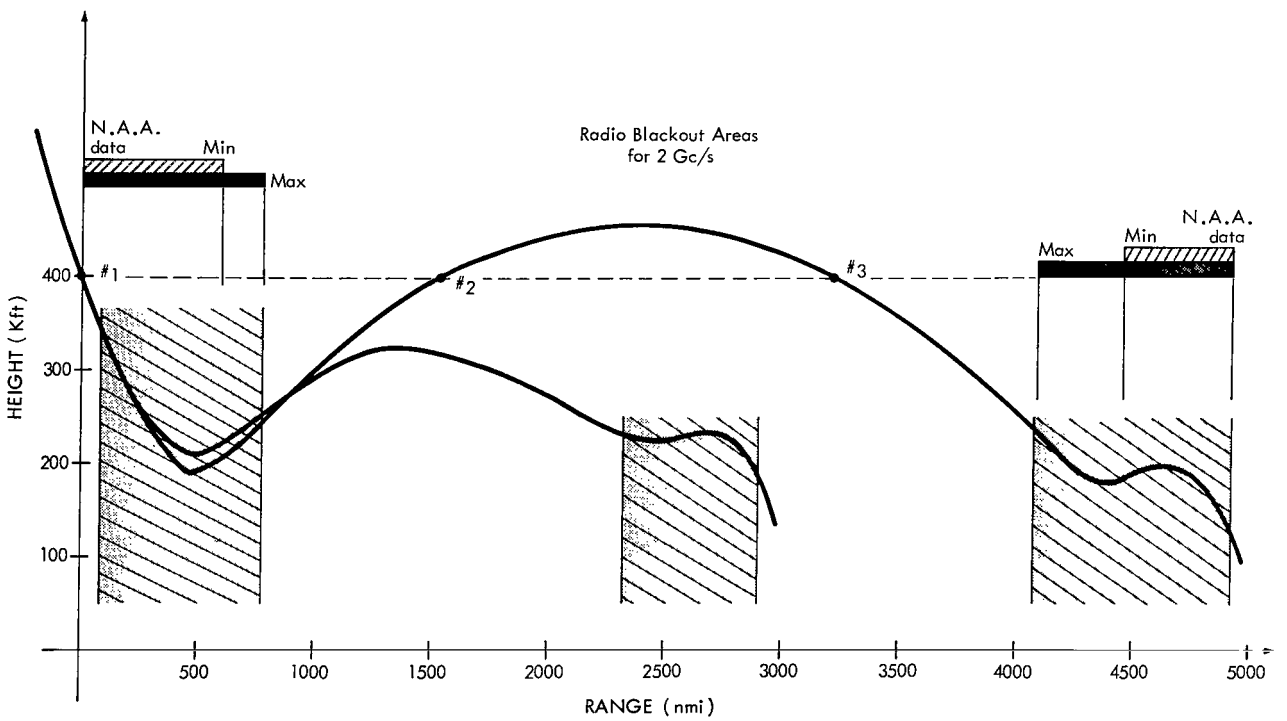

Figure 5—Apollo re-entry trajectories (vertical projection).

APOLLO RE-ENTRY TRAJECTORIES

Several Apollo re-entry trajectories have been chosen as examples in this paper (Reference 1). Typical re-entry trajectories and the possible ground tracks of concern for the Apollo with a lift-to-drag (L/D) of approximately 0.5 are shown in Figures 1 through 5. The trajectories shown in these figures (except Figure 5) have a common point #1, the first re-entry point, rather than the landing point although the latter would be more realistic. This is to show that the very first portion of the re-entry trajectories are almost independent of the range to be flown. The 5000-nautical mile trajectory shown in this figure will be considered as a "nominal" re-entry trajectory. It should be emphasized that a "standard" trajectory in the real sense does not actually exist at this time.

The particular re-entry trajectory depends on many variables such as the entry angle ranging from approximately -4.8° to -6.8° (see Figures 1 and 2), the declination of the moon (see Figures 4, 6, and 7), and the inclination of the return trajectory (40° so that the spacecraft cannot land in the cold regions of the globe under any circumstances) (Reference 1). These considerations, although somewhat variable, are applicable to a large variety of re-entry trajectories. That this is true, is important so far as a proper ground support is concerned. An effective ground tracking network

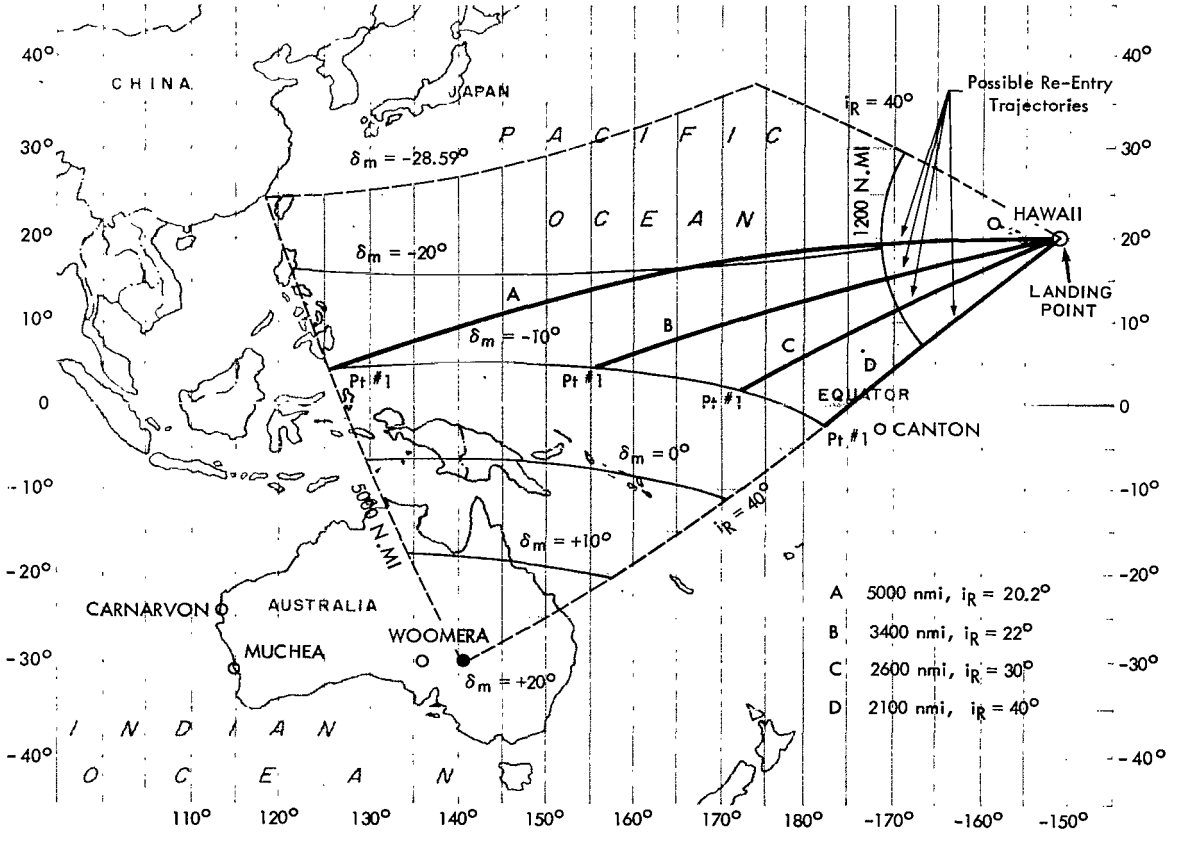

Figure 6—Locus of re-entry points (northern landing site).

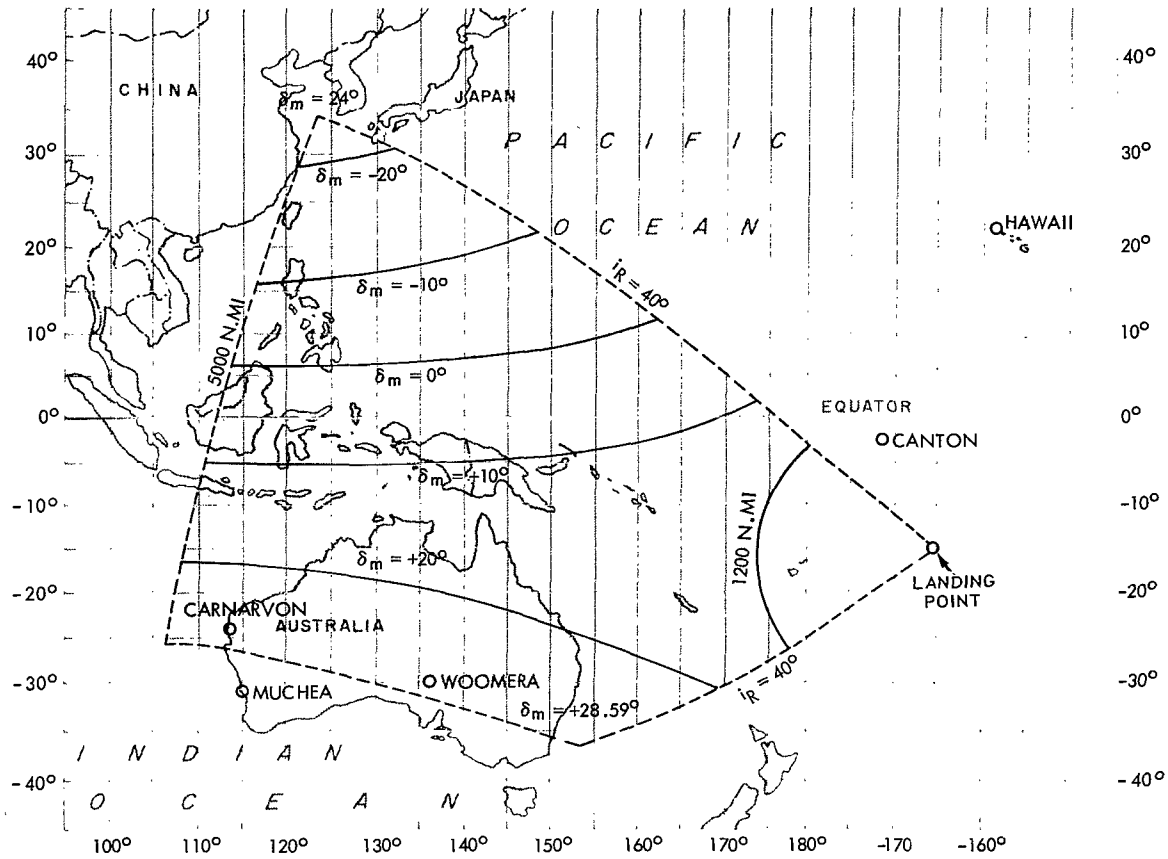

Figure 7—Locus of re-entry points (southern landing site).

must be nearly independent of the special form of the re-entry trajectory, in order to cut down the number of ground stations required. Figure 2 shows a three-dimensional schematic of the re-entry trajectories and the ground tracks of Apollo as they are depicted in Figures 1 and 3. In both graphs the fairly large lateral deviations (hundreds of nautical miles), which the spacecraft is capable of flying, are indicated.

From the above it appears almost impossible to intercept the spacecraft with a ground tracker. This, fortunately, is not so although the interception or acquisition of the re-entering spacecraft is a most serious problem. A fairly large number of variables influencing the ground tracking system are known either from the geometry of the situation or from previous measurements. Examination of Figures 4, 5, 6, and 7 helps to answer a few questions.

For any particular mission, lunar departure time, and the corresponding lunar declination (for instance -10° as shown in Figures 4, 6 and 7) are accurately known. This together with the down-range length of the re-entry trajectory determines to a certain extent the "preferred" landing site. Also known, from the mission and from tracking information during the last three days of the return flight, is the inclination i_R of the return trajectory phase within the accuracy limits of our present tracking systems and orbital theories used. Entry point #1 (Figures 1 through 6)

can be determined easily to within a few nautical miles using range, range-rate, and angle information from the Apollo tracking network.

All of this information can be used for advance planning of the location of the tracking ships and aircraft as necessary for supporting the earth re-entry portion of the lunar return.

PROBLEMS OF SPACECRAFT ACQUISITION

One of the most severe ground support problems encountered during re-entry is acquisition of the spacecraft. This can be seen by examining Figures 1, 2, 3, and 8. The maximum lateral deviations of the trajectories, as indicated in Figures 1 and 3, reach a value of approximately 700 nautical miles at a distance of 5,000 nautical miles from the first re-entry, point #1. Figure 3 also shows the circles of visibility for the ship for elevation angles $\epsilon = 10°$ (interferometer acquisition) and $\epsilon = 3°$ (communications). The circles of visibility for a spacecraft height $H = 300$ kft are left open intentionally on this figure because acquisition can be obtained only when the spacecraft is almost overhead. (See Figure 8 and Figure 3 for more details.) It further indicates the

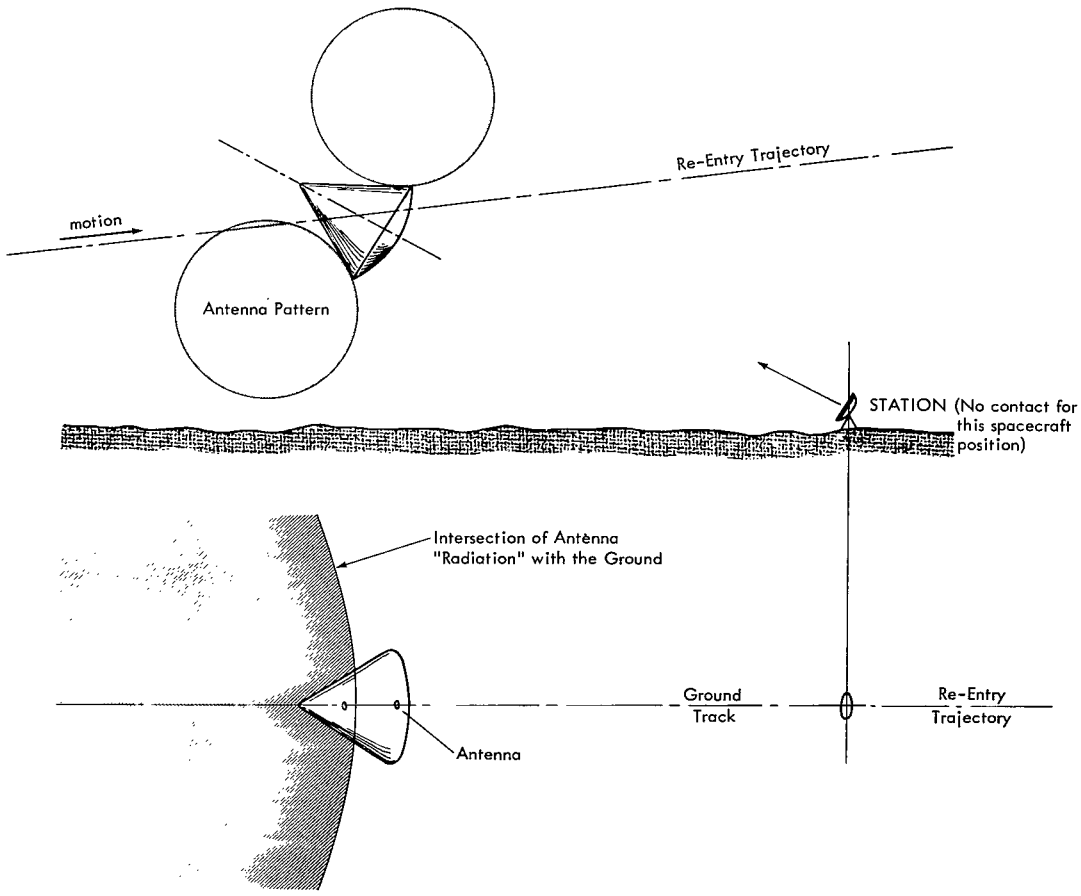

Figure 8—Radio contact for spacecraft positive lift re-entry attitude.

probability distribution of the trajectories which will be flown. This curve, contrary to all other data shown in Figure 3, is a schematic only and not a calculated one (depends on spacecraft equipment only). It should only demonstrate here that it is more probable that trajectories close to the nominal one will actually be flown, thus the interferometer circle ($\epsilon = 10°$), as shown, is adequate for acquisition. All considerations will depend on the first entry location, point #1, and adequate advance knowledge. It can be seen that an unpredicted variation of even 50 nautical miles would not harm the acquisition problem. It will be shown later that under pessimistic tracking assumptions, the orbit can be determined to adequately fix point #1.

In the following, emphasis will be placed on a special interferometric acquisition system suggested by J. T. Mengel and the author some time ago. (See Reference 2, page 13.) It is assumed that the USBS* beacon onboard the spacecraft is radiating a cw signal, that the spacecraft antennas are in operation, and that the spacecraft is beyond the blackout areas shown in Figures 1, 3, and 5.

Even under optimum conditions, it may still be impossible to contact the spacecraft by radio. Figure 6 shows the spacecraft antenna pattern for positive lift attitude. Radio contact would be obtained only when the spacecraft is almost above the tracking station, and thereafter. A "spill-over", usually not wanted from antennas in general, would be highly desirable for this special case of the Apollo antennas. Also, considerations are given to the use of IR and skin-tracking radar scanning techniques in case the spacecraft transmitter is not operating or the craft is still within the radio blackout regions. (See Figures 1, 3, and 5.) The problem of acquisition is the same in both cases since the lifting spacecraft can deviate a considerable lateral distance from the nominal track, as shown in Figures 1, 2, and 3.

To cover all flight possibilities, it is assumed that no *a priori* information is available as to when the spacecraft reaches the exit point A, A′ (shown in Figures 1 and 3). This, of course, constitutes the most undesirable case. A proper ground network must, however, cover the region of spacecraft flight capability given by γ, L/D and entry velocity v (as depicted in Figures 1, 2, and 3). Based on this, a search capability for the entire hemisphere has to be built into the tracking acquisition system. This is true for both cases, the cooperative as well as the non-cooperative systems, for acquisition. An additional requirement on these systems is short acquisition time. Short time here means time on the order of one to two seconds.

If a spacecraft height of approximately 70 km (Figures 2 and 5) and a speed on the order of 7 to 7.5 km/s during the first portion of the re-entry maneuver are assumed, a maximum angular rate (ϵ near or equal to 90°) of

$$\dot{\epsilon} \doteq \frac{v}{h} \doteq \frac{1}{10} \text{ rad/sec} \doteq 6°/\text{sec} \qquad (1)$$

*USBS stands for Unified S-Band System. This system combines tracking (range, range-rate, and JPL's pseudo random code) and communications into a single system for both tasks.

is to be expected (Figure 8). If the position of the spacecraft and its possible great angular speed (if overhead) are unknown, real problems for spacecraft acquisition are created.

SPECIAL RE-ENTRY ACQUISITION SYSTEMS

Taking into account the existing acquisition problems after re-entry (see point #2 in Figures 1 and 5) led to the concept of using an interferometer with fixed, broad beam antennas as an acquisition aid. The advantage of such an instrument, provided in over six years of operation of the Minitrack system, is that no moving antennas such as in the case of search radars are required and that nearly hemispherical coverage (10° above horizon) can be obtained (Figure 9).

Assuming that the spacecraft USBS transmitter radiates a cw signal, the omnidirectional individual interferometer antennas can receive this signal from which the phase difference ϕ can be determined using phase measuring techniques (References 3 through 7 and 8 for more details).

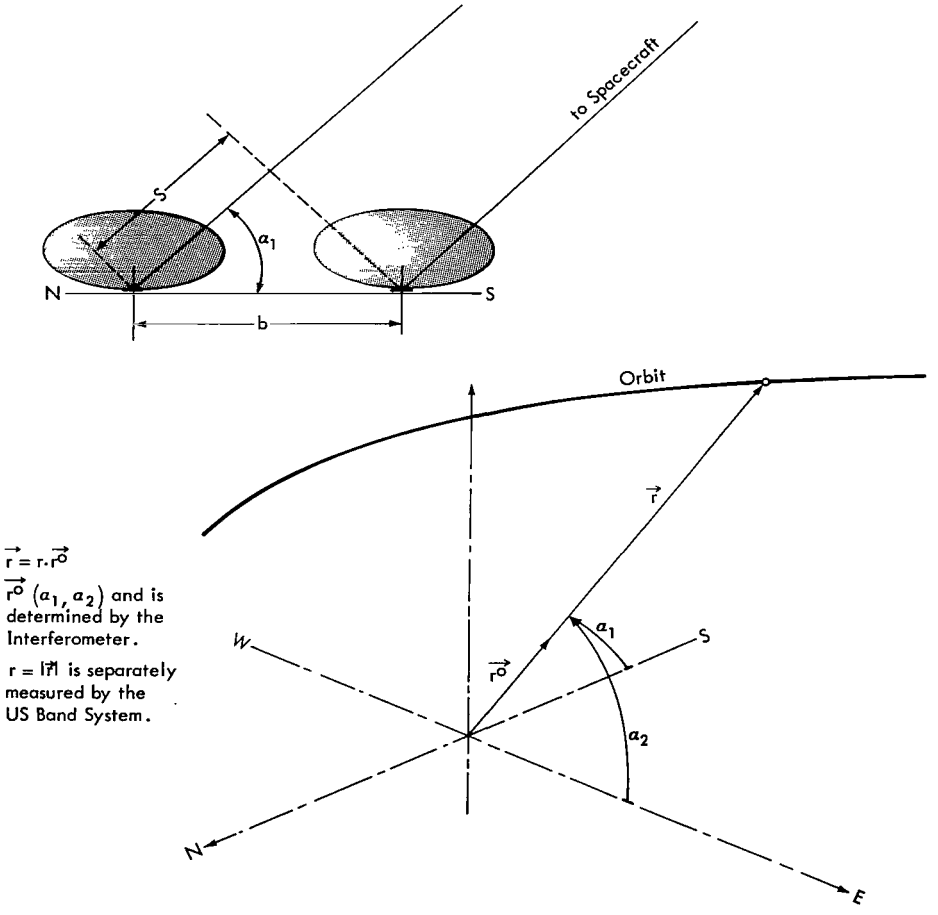

Figure 9—Schematic of re-entry interferometer antennas.

From this phase

$$\phi = 2\pi \frac{s}{\lambda} , \tag{2}$$

the angle α_1 (shown in Figure 9) can be determined by

$$\cos \alpha_1 = \frac{s}{b} = \frac{\phi\lambda}{2\pi b} , \tag{3}$$

knowing the wavelength λ, the antenna separation b and the phase difference ϕ (measured) and where s is the wavefront separation distance. The angles α_1 between the position vector of the spacecraft $\vec{r}$ and the N-S baseline and α_2, the equivalent in the E-W direction, determine the local unit position vector $\vec{r}^\circ$ of the spacecraft.

This determination of $\vec{r}^\circ$ solves the acquisition since, with this knowledge, a small dish can be directed toward the spacecraft to accomplish a range measurement r and also to establish communications.

The local spacecraft position vector $\vec{r}$ is then given by

$$\vec{r} = r \cdot \vec{r}^\circ \tag{4}$$

and this spacecraft position vector can be used to check the spacecraft re-entry trajectory $\vec{r} = f(t)$.

Before continuing it may be appropriate to derive some of the major design parameters for such a re-entry interferometer. Varying Equation 3 with respect to ϕ, λ, and b, and collecting terms results in

$$\delta\alpha_1 = \frac{1}{2\pi \sin\alpha_1} \left(\frac{\lambda}{b}\right) \left[\delta\phi + 2\pi \left(\frac{b}{\lambda}\right) \cos\alpha \left(\frac{\delta\lambda}{\lambda} - \frac{\delta b}{b}\right)\right] \tag{5}$$

The frequency (wavelength) can be considered as constant during the time the wave reaches the two interferometer antennas, that is, $\delta\lambda = 0$; one then obtains from Equation 5 the following error in α_1 using the Gaussian principle of propagation of errors.

$$\sigma_\alpha = \frac{1}{2\pi \sin\alpha} \sqrt{\left(\frac{\lambda}{b}\sigma_\phi\right)^2 + \left(2\pi \cos\alpha \frac{\sigma_b}{b}\right)^2} \tag{6}$$

Utilizing a proper "balance" between the obtainable errors, σ_ϕ in the electrical phase measurement and σ_b in the baseline length, one obtains for σ_α the following values with 1 (see Reference 3

for more details)

$$\left.\begin{aligned} \lambda &= 15\ \text{cm}, \quad b = 1.5\text{m}, \quad \frac{\lambda}{b} = \frac{1}{10} \\ \sigma_\phi &= \frac{1}{57}\ \text{rad}\ (\sim 1^\circ), \quad \sigma_b = 0.1\ \text{cm} \end{aligned}\right\} \tag{7}$$

$$\text{for } \alpha = 90^\circ \cdots \sigma_\alpha = 0.5\,\text{mrad}; \quad \alpha = 10^\circ \cdots \sigma_\alpha = 5\,\text{mrad}\ .$$

Figure 10 shows the expected angular error σ_α in mrad as a function of the angle α for an assumed electrical phase-measuring error of 1° and baseline-length errors of 1, 2, and 3 mm as indicated on the graph. These angular errors will be used later to estimate the errors of the skipout trajectory and thus those of the second re-entry point (point #3 in Figures 1, 5, and 11).

An interferometer of this kind, designed especially for re-entry acquisition of the Apollo spacecraft, is presently under construction at Goddard. It is planned that the ground plane

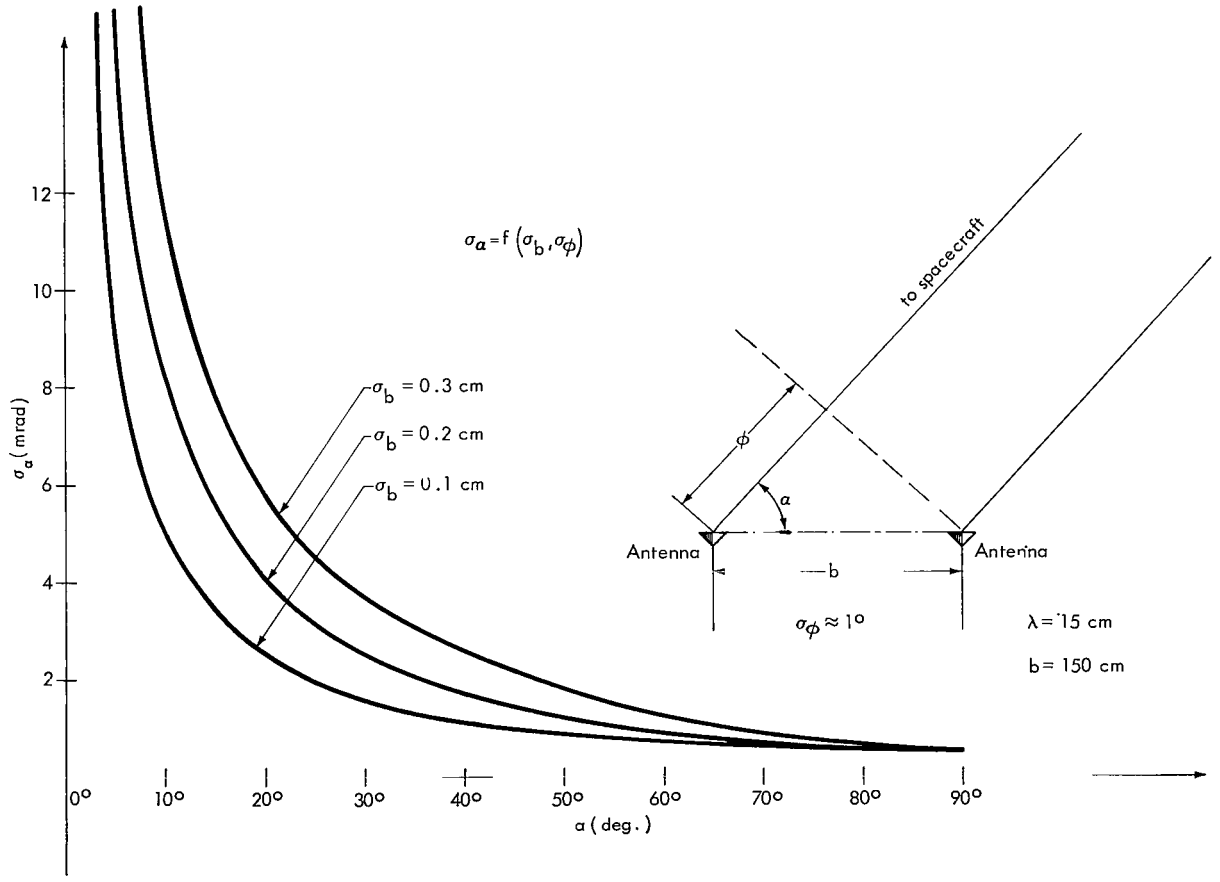

Figure 10—Interferometer angular errors.

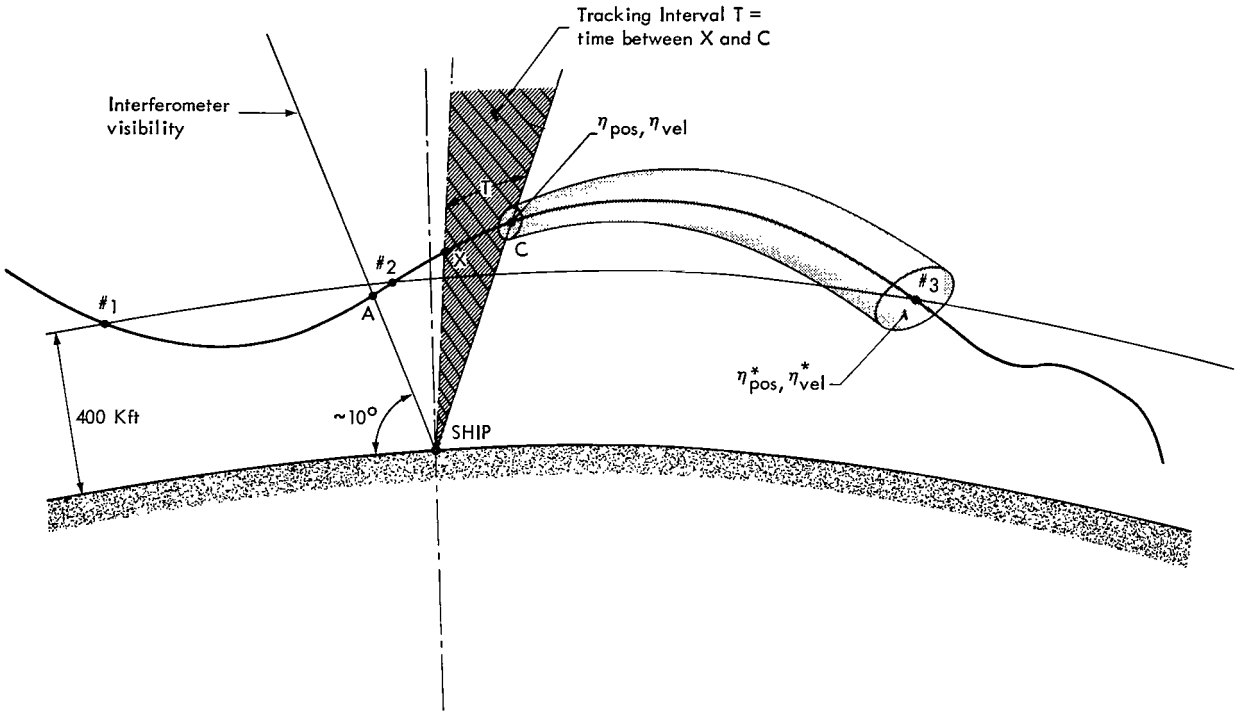

Figure 11—Schematic of re-entry tracking and error projection.

accommodating both perpendicular base lines (Figure 9) as well as all the ambiguity antennas will measure less than approximately 10' × 10'. The output of this interferometer will be the equivalent to angles α_1 and α_2 as shown in Figure 9 (that is the unit position vector $\vec{r}^\circ$ from the ground station to the spacecraft) as well as their rates $\dot{\alpha}_1$ and $\dot{\alpha}_2$ (or $\dot{\vec{r}}^\circ$).

TRACKING STATION LOCATIONS ALONG THE RE-ENTRY GROUND TRACK

The next step is to show the optimum position (location with respect to the lifting re-entry trajectory) for a ground tracking station (ship) in order to support the entering lunar spacecraft. (Position here means the location of the tracker on earth in respect to the lifting re-entry trajectory.) Figure 12 shows the position of the re-entry ship and of the aircraft necessary to support the re-entering spacecraft with communication capability. The same aircraft are being used that were used for injection (communications coverage during the transition from the parking orbit to the lunar transfer orbit). They are depicted in Figure 12 only to show that 5 aircraft together with the necessary re-entry ship can cover the total 5,000-nautical mile re-entry track. Removing aircraft A_2 or A_3 will still allow coverage of most of the trajectory (marginal but sufficient if only four aircraft are available).

For any mission the lunar take-off time, the declination of the moon δ_m, the planned inclination i_R of the return trajectory (Figure 4), and the time characteristic are known. The earth landing site can be chosen from this data (References 1 and 2). Figures 6 and 7 show the areas of first

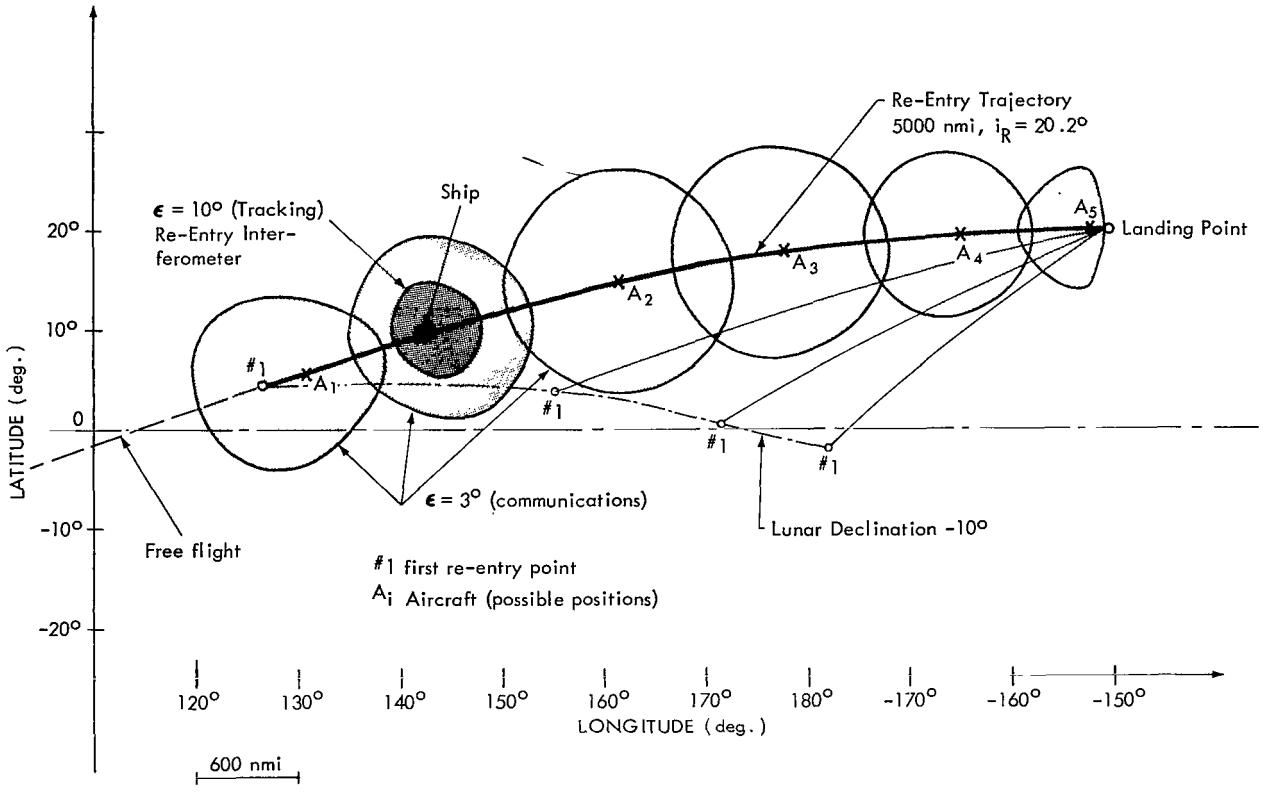

Figure 12—Apollo re-entry tracking and communications.

re-entry (point #1) for northern and southern landings. It should be noted that the landing points finally chosen will not greatly alter the considerations here since the coverage which has to be provided by the re-entry network using ships and aircraft is fairly independent of the particular landing point chosen for the real mission. Tracking information collected during the 70-hour return flight will be used to alter the return trajectory by using proper midcourse maneuvers to assure that the first re-entry point coincides with that previously planned.

Figure 13 depicts a possible return trajectory for landing in the Hawaiian area. This trajectory is used as an example to show that tracking information using only the Canberra 85' dish and the Indian Ocean ship's* 30' dish is adequate for our impact point #1 determination. It is assumed here (pessimistically) that tracking information for orbit determination is not available from distances beyond 51,000 nautical miles (8 hours before entry). With one 85' dish (when the spacecraft is still a few hours out) and one 12' or 30' dish (on the Indian Ocean ship), tracking is adequate to locate the spacecraft in advance of re-entry (Figure 12). Even without this ship the entry, point #1, would be known well enough for this purpose. It should be emphasized that these loose requirements here are only related to the re-entry ships location and acquisition problem

*This ship is located at approximately 38°E and 18°S (off Madagascar) to cover the post injection phase (7 min. coverage) and can be moved during the seven days of the mission to a location of approximately 90°E and 10°S (S. W. of Indonesia) to cover the approaching spacecraft for minutes (6 to 7 min.) before it reaches the atmosphere at 400 kft.

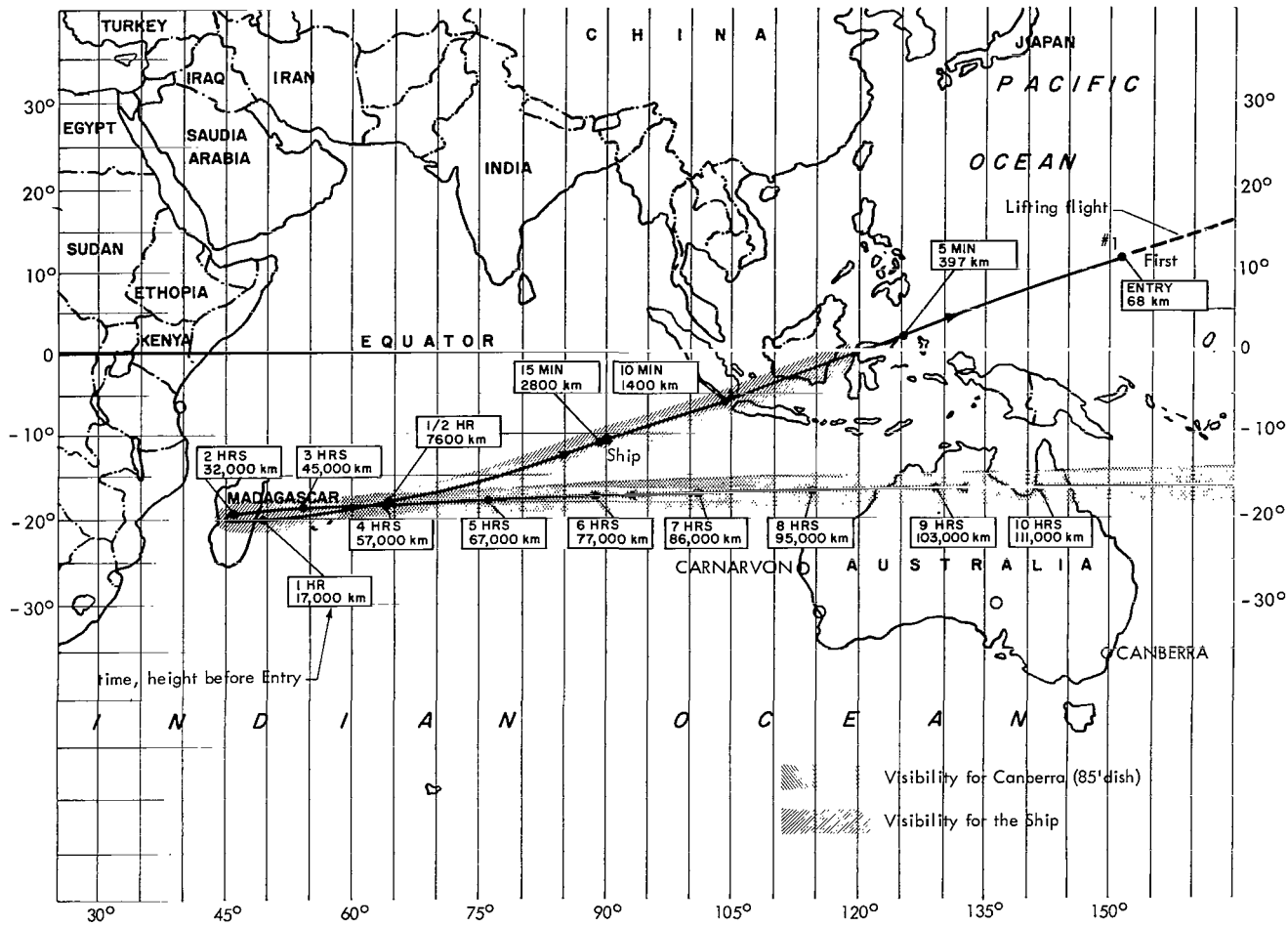

Figure 13—Example of a lunar return trajectory (i_R = 20.1°).

and not to the tighter requirements from the aerodynamic re-entry point of view. The re-entry angle, for instance, is a critical parameter as far as atmospheric re-entry is concerned (References 11, 12, and 13). Figure 14 shows the errors associated with the entry under the loose conditions stated above. A tracking sampling rate of one range, range-rate, azimuth and elevation measurement per minute is assumed.

Figure 6 shows the locus of the re-entry points (designated as #1 in Figures 1 through 7) for a Hawaiian water landing. The only limitations given are those of the lunar declinations δ_m, the maximum re-entry range of 5000 nautical miles and the maximum inclination of the lunar return trajectory i_R = 40°. The reason for this is to assure that the spacecraft will not land in the cold regions of the earth (assumed to be above 40° latitude) under any circumstances. Figure 7 shows a similar graph for a southern landing.

Figure 12 (clarifying details of Figures 4 and 6) shows the possible re-entry trajectory for δ_m = -10° and a return inclination i_R = 20.2°. In this case, it can be seen that only the i_R = 20.2° return trajectory would be 5,000 nautical miles long (assuming that the landing point is given for

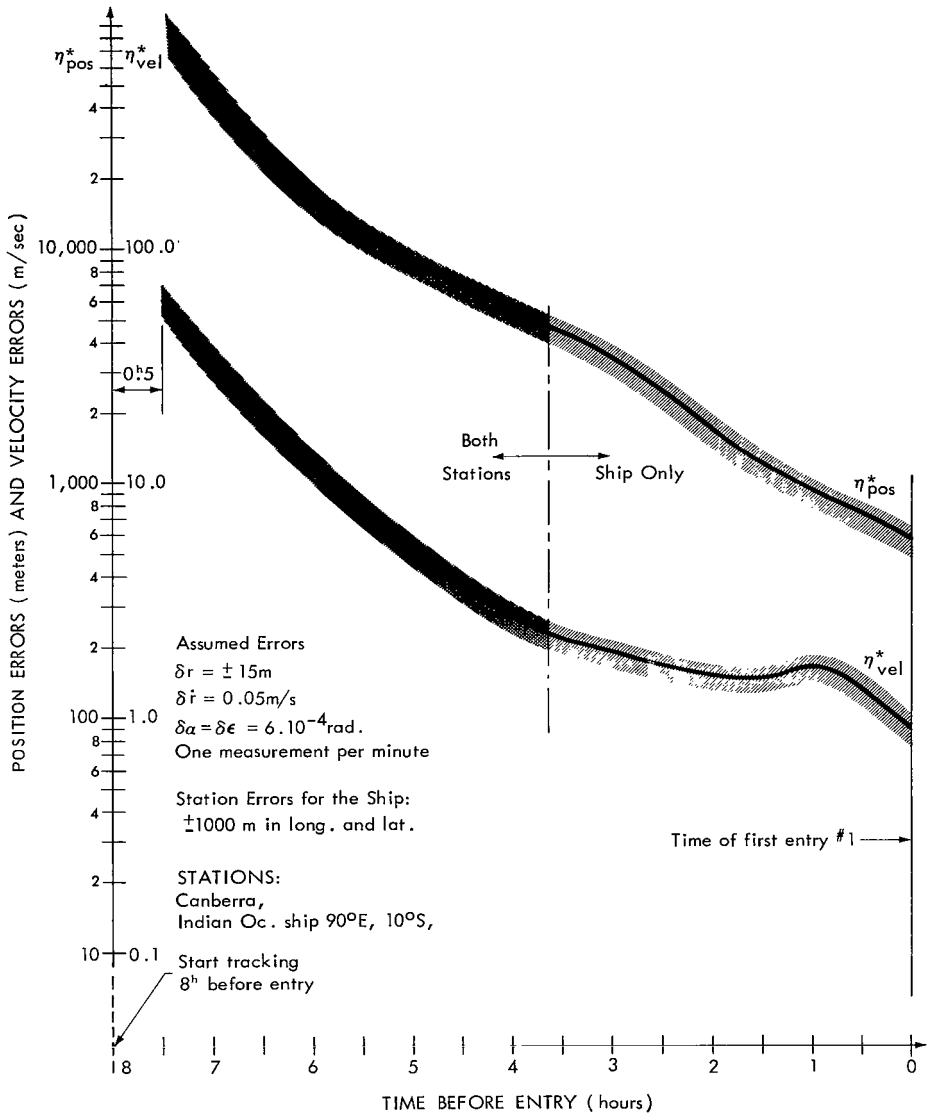

Figure 14—Position and velocity errors predicted to the entry point #1.

different return inclinations*). Using this example, the tracking ship would have to be placed approximately 1,000 nautical miles down range from point #1 as indicated in the previous graphs.

The odd shaped areas of coverage for tracking (elevation angle $\epsilon = 10°$) for the interferometer on the ship (dark area) and communications ($\epsilon = 5°$, aircraft height $\doteq$ 30,000 ft.) are due to the height variation of the spacecraft flying the re-entry trajectory shown in Figure 1. Comparison of the dark area representing the tracking capability of the ships acquisition interferometer ($\epsilon = 10°$),

*The following simplifying assumptions have been made (Reference 2, p-2): constant earth moon distance; a constant vacuum perigee; a constant true anomaly of 174°; only the earth's gravitational field acting on the vehicle.

and the maximum deviation of the spacecraft depicted in Figures 1 and 3, show that acquisition should be possible under any circumstances. The "final" position of the ship will depend on the real blackout areas (which will be better determined than at present) and the real lateral flight capability of the spacecraft. Figure 3 gives a better view of the beginning of the re-entry phase. As shown here, the ship is placed just "outside" of the blackout area approximately 1,000 nautical miles downrange from point #1.

Communications Blackouts

Blackout areas are considered to be those areas along the re-entry trajectory where the electron density is so high that communication between the re-entering spacecraft and a ground station is impossible. The frequency regions considered for this definition are those commonly used for communications up to 10 kmc (Reference 14). The reason for the increased electron density in the vicinity of the entering spacecraft is the transfer of the kinetic energy of the spacecraft (by braking action of the upper region of earth's atmosphere) into heat, predominently by compression in the stagnation region but partially by skin friction in the boundary layers. Figures 1, 3 and 5 show these areas of radio blackout from Apollo-type vehicles (Reference 12). As can be seen from Figure 5, considerable differences exist (up to about 400 nautical miles) in the extent of these regions, indicating that more studies are required to clearly define them. As indicated in the graph, up to 50% of the total communications time may be lost due to an extension of the blackout region.

Tracking Acquisition Angle

The tracking ship and its acquisition problems will now be considered. The ship's initial acquisition angle $\left(\alpha_{s_{in}} = 75^{\circ}\right)$ is indicated in Figure 3. Immediate acquisition is difficult to get due to the antenna pattern and the attitude of the spacecraft. As shown in Figure 8, antenna "spill-over" may be enough to make acquisition possible. This in turn suggests a non-directional spacecraft antenna design. The spacecraft could emerge within an angle of 75° at minimum, taking the worst condition of a short and one-sided trajectory (maximum deviations of the ground track end-points). In case acquisition is not immediate, the angle $\alpha_{s_{in}}$ could increase to *almost* 180° (since the interferometer minimum elevation angle is approximately 10°). By placing the ship in the indicated position, it is assured that the "ship visibility" exceeds the maximum lateral maneuverability of the spacecraft as indicated in Figure 3.

Spacecraft Position and Velocity Errors

Assume, now, that the spacecraft has been acquired at a point X and that it is tracked over a period of time T during its "free-flight" skipout as shown in Figure 11 (compare with Figure 1). The questions arise: what error in spacecraft position and velocity $(\eta_{pos}$ and $\eta_{vel})$ can be determined in the vicinity of point C when the spacecraft leaves the visibility region of the ship, and what is the magnitude of the projected errors $(\eta^*_{pos}$ and $\eta^*_{vel})$ to the second re-entry point, point #3. Figures 15 and 16 answer these questions by utilizing tracking information from the ship's USBS system (with and without ship location errors).

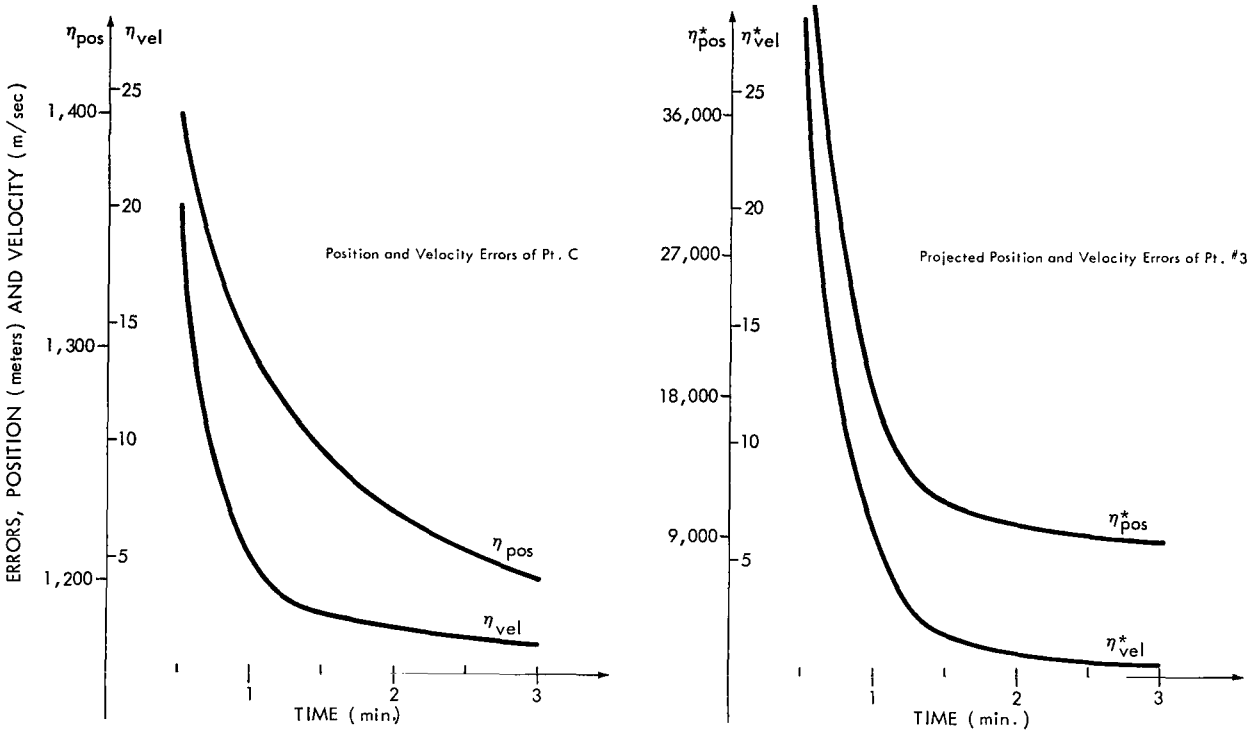

Figure 15—Re-entry tracking errors and their projections (ships position errors of ±1 km in lat. & long.).

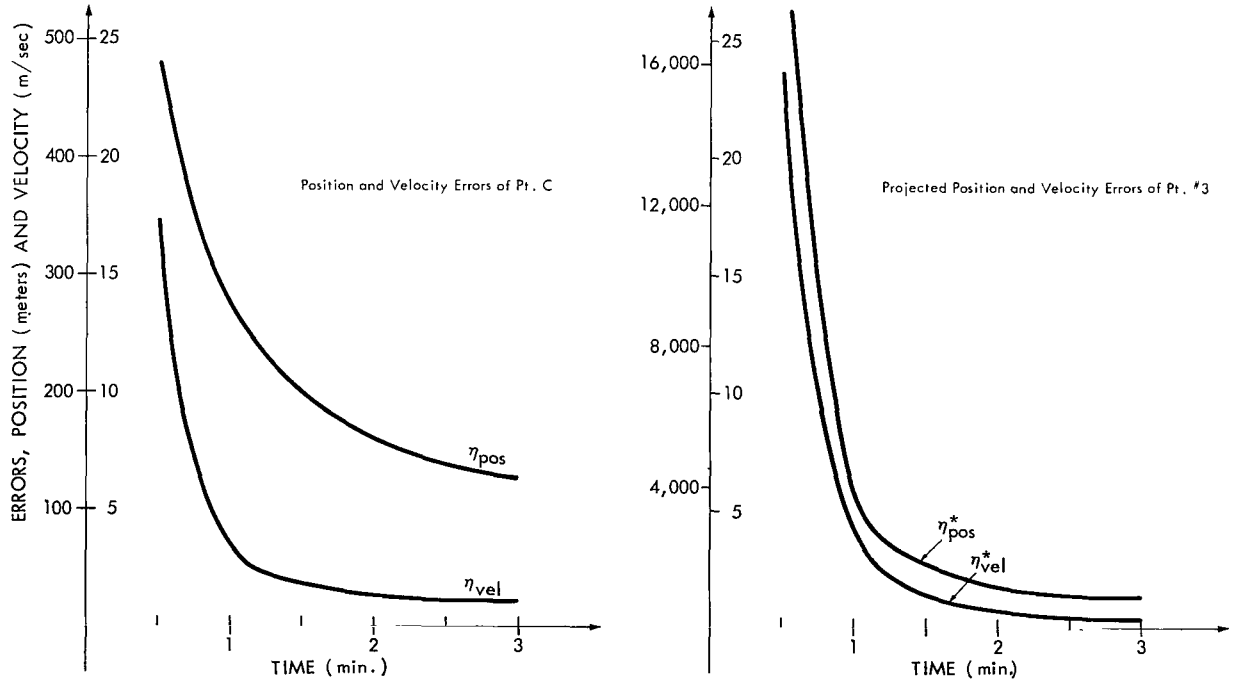

Figure 16—Re-entry tracking errors and their projections (no ships position errors).

An error in the location of the ship of ±1 km in latitude and longitude has been assumed for the calculations depicted in Figure 16 (References 13, 14 and 15). Figures 15 and 16 show both the position and velocity errors at the end of the tracking as well as the projection of these errors to the second re-entry. For short tracking times on the order of seconds, acquisition has been accomplished relatively late (acquisition point X is near C in Figure 11); the errors are relatively large, and so are their projections to point #3. Nevertheless, all are within the limits of the spacecraft dynamic flight capability. For example, if it is assumed that errors in the location of the ship are within ±1000 meters (3,300 feet) in longitude and latitude and late acquisition allows only 40 seconds for tracking, then the errors are η_{pos} = 1360 meters and η_{vel} = 11 meters/second, and their projections are η^*_{pos} = 34,000 meters and η^*_{vel} = 15 meters/second (as seen from Figure 16).

Ship Prepositioning

Since the ship is prepositioned during the last few hours of the mission (because of its slow velocity) and can be considered a fixed station (Figures 1, 3, and 12), certain precautions for proper re-entry coverage have to be taken. These precautions impose no limitations on the mission. To assure that the ship can acquire the spacecraft despite variations due to "last minute" spacecraft maneuvers, changes of the entry point #1 are considered. These variations along, and perpendicular to, the re-entry track can be expressed in a simple form by:

$$\left.\begin{aligned} \delta_{perp} &\doteq \frac{(R+h)}{v_o \cos \gamma_o} \cdot \delta v_{o_{perp}} \\ \text{and} \\ \delta_{track} &\doteq \frac{(R+h)}{\gamma_1} \sqrt{\frac{2r_o}{\mu}}\, \delta v_{o_{track}} \end{aligned}\right\} \qquad (8)$$

where R is the earth radius, h is the height of the re-entry point above earth, γ_o is the flight path angle for r_o and v_o, v_o is the velocity where a velocity maneuver of $\delta v_{o_{perp}}$ or $\delta v_{o_{track}}$ is to be executed at a distance r_o from the center of the earth, μ is the gravitational parameter, and γ_1 is the re-entry flight path angle (-5° to -7°). Equations 8 are based on simple Keplerian orbits using the earth as the only attracting body. Varying these orbital equations with respect to the velocity and neglecting higher order terms result in the Equations 8 stated above, giving the variations perpendicular to and along the re-entry track. Figures 17 and 18 present Equations 8 in graphical form. These figures indicate that it is unnecessary to alter the ship's position for "wrong maneuvers" in the perpendicular direction such as: changes in spacecraft velocity $(\delta v_{o_{perp}})$ up to 9 feet/second, time to re-entry up to 4-1/2 hours, or range as great as 32,500 nautical miles. From Figure 18 it can deducted that a "wrong" change in velocity along the tangent $\delta v_{o_{tang}} \doteq 9$ ft/s performed 4-1/2h out would result in a change $\delta_{track} \doteq 60$ nautical miles for the re-entry point #1,

which also is not dangerous from the ground tracking point of view since it would only result in a tracking time loss of approximately 10 seconds. Not "recorded" variations $\delta v_{o_{track}}$ $\doteq$ 30 ft/s as much as 10h out ($r_o \doteq$ 64,000 nautical miles) would on the other hand, reduce the tracking ship's usefulness since the change of $\delta_{track} \doteq$ 270 nautical miles would bring the blackout region beyond the tracking ship as shown in Figures 1 and 3. Even under these conditions, not too much harm would be done. This shows that the prepositioning of the ship is indeed possible.

Figures 17 and 18 also show what changes in point #1 (on earth) can be accomplished when tracking data (hence the nominal return trajectory) indicate that the actual location of this point is not where previously planned, therefore, these figures may be used to optimize the ground tracking capability.

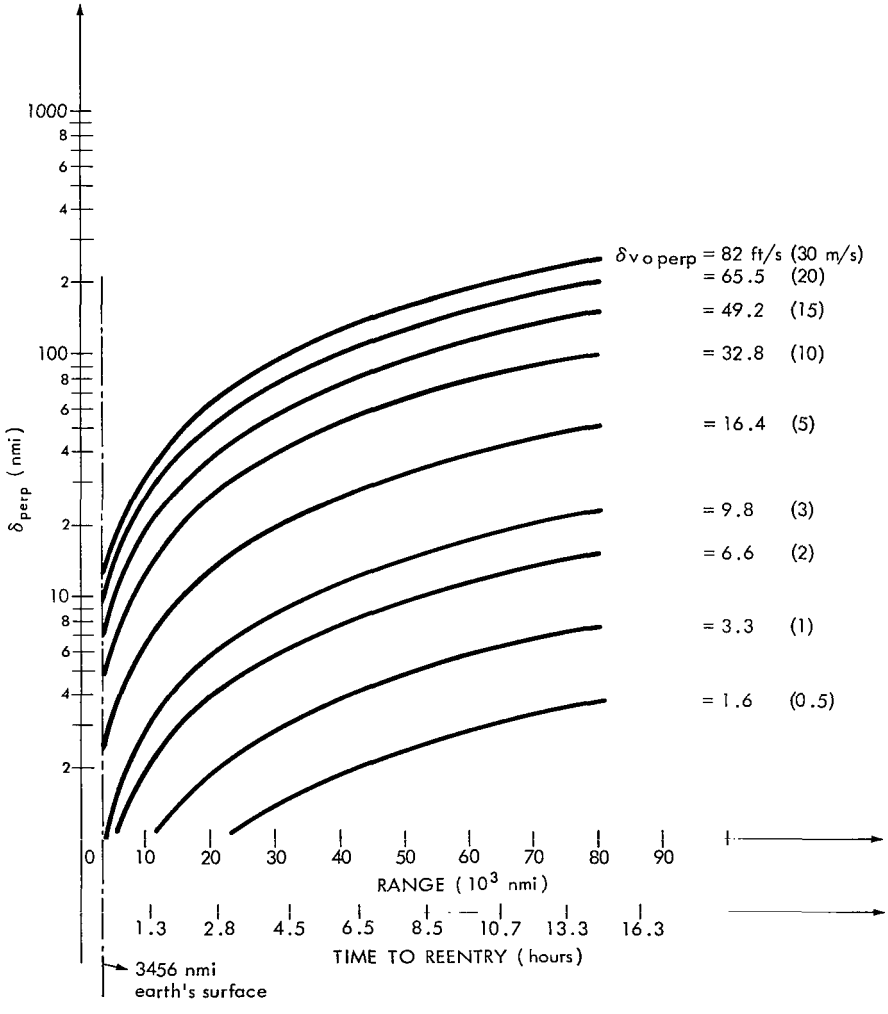

Figure 17—Variations of the entry point perpendicular to the track.

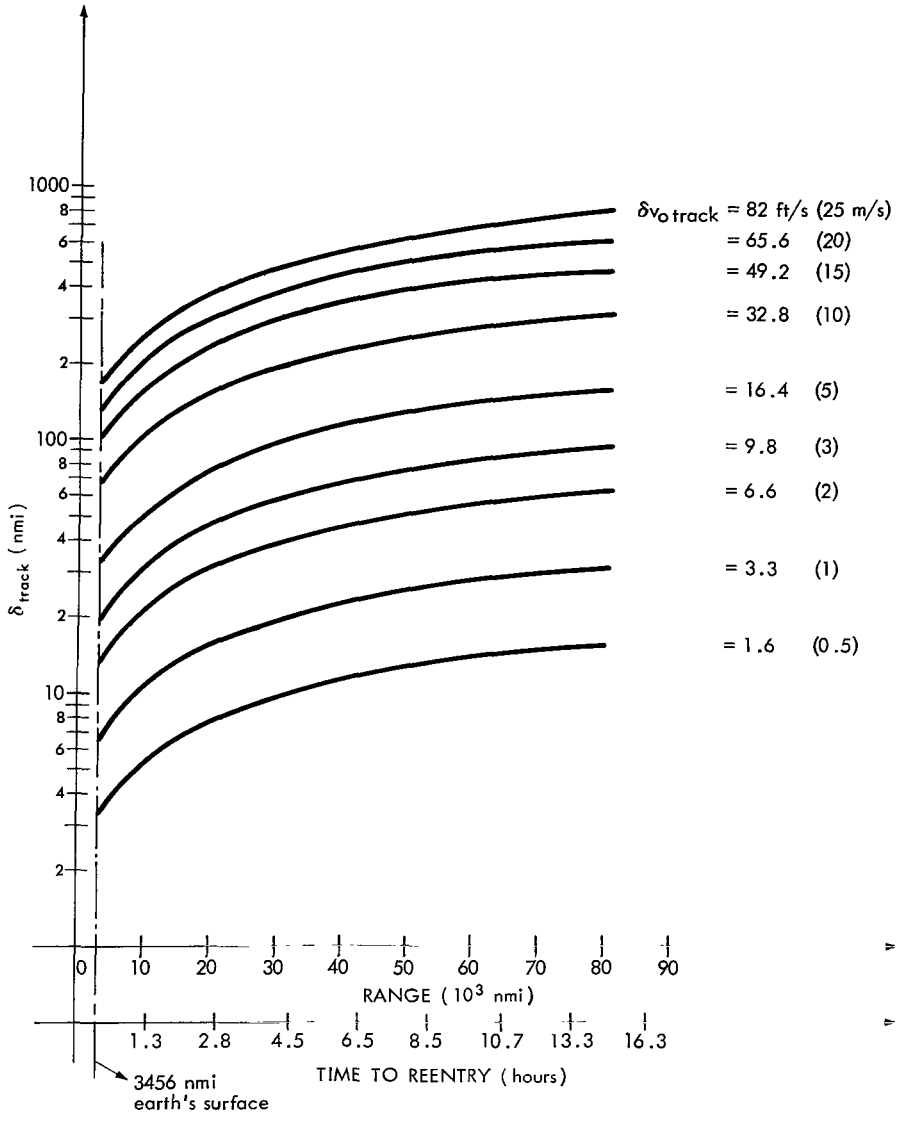

Figure 18—Variations of the entry point along the track.

CONCLUSION

As mentioned in the course of this paper, Goddard has built a breadboard model of a re-entry interferometer (acquisition system for the USBS). The ground plans dimensions are approximately 10' × 10'. Four racks of electronic equipment, with a display console, constitute the total system. It is anticipated that this breadboard model will be in operation by July 1964. At this time it is planned to perform aircraft tests using one of Goddard's calibration airplanes (DC-6). A USB-transponder and proper antennas will be installed in the aircraft to simulate acquisition and study the problems in more detail.

Studies are also under way at Goddard (Reference 16) to investigate the possibility of utilizing the generated re-entry heat (infrared) to acquire the spacecraft. This is of importance particularly for aircraft in order to direct the USB antennas toward the entering spacecraft to establish communications. Also here hemispherical search capability is of importance in order to cover all possible re-entry flights during the spacecraft's early dynamic and ballistic (skip) paths.

As mentioned also, radio blackout, particularly its beginning and ending period during certain portions of the re-entry flight constitute a problem. In order to gain more insight in this area, Goddard Space Flight Center and The Cornell Aeronautical Laboratory* will continue the theoretical investigation of more sophisticated mathematical models of ionized flow field and radio frequency propagation through this flow field during super orbital re-entries into the earth's atmosphere. Actual radio wave propagation measurements will also be performed in the well-surveyed flow field surrounding the model under simulated transmitting conditions of the re-entering spacecraft. Experiments to study ablation effects, fluid injection and local magnetic fields surrounding the antenna (control of the tensor characteristic of the plasma) will also be investigated experimentally at Cornell. It is hoped that with this two-pronged approach, real progress can be made toward a solution of the blackout problem acceptable to the final operation during re-entry of this last phase of the lunar mission.

ACKNOWLEDGMENT

The author wishes to acknowledge the assistance of Mr. J. T. Mengel in reviewing this report and Mrs. A. Marlow, Mr. T. Jones, Mr. R. Groves and in particular Mr. W. Kahn in the preparation of it. In addition the author wishes to thank Mr. L. Jenkins, Mr. J. Hodge, Mr. J. Mayer, and Mr. C. Kraft of the Manned Spacecraft Center for their helpful discussions on this subject.

(Manuscript Received November 17, 1964)

REFERENCES

1. , "Trajectory Studies for Use in Determining Tracking Requirements for Project Apollo." Manned Spacecraft Center, Flight Operations Division, Mission Planning Department, August 30, 1963.

2. Vonbun, F. O., "Parking Orbits and Tracking for Lunar Transfers." Goddard Space Flight Center Document X-520-62-63, June 7, 1962.

3. Simas, V. R., "A System for Re-Entry Tracking of the Apollo Spacecraft." Goddard Space Flight Center Document X-523-63-56, April 2, 1963.

4. Schroeder, C. A., Looney, C. H., Jr., and Carpenter, H. E., Jr., "Tracking Orbits of Man-Made Moons." *Electronics*, Vol. 32, no. 1, pp. 33-37, January 2, 1959.

*Buffalo, New York.

5. Mengel, J. T., "Minitrack System Design Criteria." *Electrical Engineering,* Vol. 76, no. 8, pp. 667-672, August 1957.

6. Mengel, J. T., "Tracking Earth Satellite and Data Transmission by Radio." *Proceedings of the Institute of Radio Engineers,* Vol. 44, no. 6, pp. 755-760, June 1956.

7. Simmons, G. J., "A Theoretical Study of Errors in Radio Interferometer Type Measurements Attributable to Inhomogeneities of the Medium." *IRE Transactions on Telemetry and Remote Controls,* Vol. TRC3, no. 3, pp. 2-5, December 1957.

8. , "Phase Measurement and Display Subsystem for Apollo Re-Entry Tracking System." Goddard Space Flight Center Document X-531-63-251, December 13, 1963.

9. Young, J. W., Russel, W. R., "Fixed-Base Simulator Study of Piloted Entries into the Earth's Atmosphere of a Capsule-Type Vehicle at Parabolic Velocity." NASA Technical Note D-1479, October 1962.

10. Assadourian, A., Cheatham, D. C., "Longitude Range Control During the Atmospheric Phase of a Manned Satellite Re-Entry." NASA Technical Note D-253, May 1960.

11. Foudriat, E. C., Wingrove, R. C., "Guidance and Control During Direct Descent Parabolic Re-Entry." NASA Technical Note D-979, November 1961.

12. Lehnert, R. L., Rosenbaum, B., "Plasma Effects on Apollo Re-Entry Communications." Goddard Space Flight Center Document X-513-64-8, January 1964.

13. Vonbun, F. O., Kahn W. D., "Tracking Systems, Their Mathematical Models and Their Errors." Part I—Theory, NASA Technical Note D-1471, October 1962.

14. Kahn, W. D., Vonbun, F. O., "Tracking Systems, Their Mathematical Models and Their Errors." Part II—Least Square Treatment, to be published soon as a NASA Technical Note.

15. Cooley, C. L., "Tracking Systems, Their Mathematical Models and Their Errors." Part III—Program Description, Goddard Space Flight Center Document X-513-64-145, May 20, 1964.

16. Plotkin, H. H., "Infrared Re-Entry Tracking" Goddard Space Flight Center Document X-524-62-136, August 10, 1962.

17. , "A Ground Instrumentation Support Plan for the Near-Earth Phases of the Apollo Mission." Goddard Space Flight Center Document X-520-62-211, November 23, 1962.

Appendix A

List of Symbols Used

Symbol	Meaning
D	Drag on re-entry vehicle
H	Spacecraft height
L	Lift on re-entry vehicle
L/D	Lift-to-drag ratio
R	Earth radius
T	Tracking time
b	Interferometer tracking antenna separation distance
h	Height of spacecraft entry point
i_R	Inclination of return trajectory
$\vec{r}$	Position vector of spacecraft
$\vec{r}^{\circ}$	Local unit position vector of spacecraft
$\dot{\vec{r}}^{\circ}$	Unit position-vector rate
r_o	Range of spacecraft from center of earth
s	Interferometer antenna wavefront separation
v	Spacecraft entry velocity
v_o	Spacecraft velocity during $\delta v_{o_{perp}}$ or $\delta v_{o_{track}}$
α_1	Angle (degrees) between spacecraft position vector $\vec{r}$ and N-S baseline
α_2	Angle (degrees) between spacecraft position vector $\vec{r}$ and E-W baseline
$\dot{\alpha}_1$	Angular rate for α_1
$\dot{\alpha}_2$	Angular rate for α_2

$\alpha_{s_{in}}$ Ship's initial horizontal acquisition angle (degrees)

γ Spacecraft flight-path re-entry angle (degrees)

γ_o Flight path angle (degrees) for r_o and v_o

δ_m Lunar declination (degrees)

δ_{perp} Change in re-entry point perpendicular to re-entry track

δ_{track} Change in re-entry point parallel to re-entry track

$\delta v_{o_{perp}}$ Change in spacecraft velocity perpendicular to re-entry track

$\delta v_{o_{tang}}$ Change in spacecraft velocity along tangent line

$\delta v_{o_{track}}$ Change in spacecraft velocity parallel to re-entry track

$\delta\alpha_1$ Change in angle between spacecraft position vector $\vec{r}$ and N-S baseline

$\delta\lambda$ Wavelength difference at interferometer receiving antennas

$\delta\Phi$ Change in phase difference (interferometer)

ϵ Elevation angle of tracking antennas (degrees)

$\dot{\epsilon}$ Angular rate for ϵ

η_{pos} Tracking error in spacecraft position at first re-entry point, point #1

η^*_{pos} Tracking error in spacecraft position projected to second re-entry point

η_{vel} Tracking error in spacecraft velocity at first re-entry point, point #1

η^*_{vel} Tracking error in spacecraft velocity projected to second re-entry point

λ Interferometer tracking wavelength

μ Gravitational parameter

σ_α Angular error (milliradians)

σ_b Baseline length error

σ_ϕ Electrical phase error (radians)

ϕ Phase difference (interferometer)

"The aeronautical and space activities of the United States shall be conducted so as to contribute . . . to the expansion of human knowledge of phenomena in the atmosphere and space. The Administration shall provide for the widest practicable and appropriate dissemination of information concerning its activities and the results thereof."

—NATIONAL AERONAUTICS AND SPACE ACT OF 1958

NASA SCIENTIFIC AND TECHNICAL PUBLICATIONS

TECHNICAL REPORTS: Scientific and technical information considered important, complete, and a lasting contribution to existing knowledge.

TECHNICAL NOTES: Information less broad in scope but nevertheless of importance as a contribution to existing knowledge.

TECHNICAL MEMORANDUMS: Information receiving limited distribution because of preliminary data, security classification, or other reasons.

CONTRACTOR REPORTS: Technical information generated in connection with a NASA contract or grant and released under NASA auspices.

TECHNICAL TRANSLATIONS: Information published in a foreign language considered to merit NASA distribution in English.

TECHNICAL REPRINTS: Information derived from NASA activities and initially published in the form of journal articles.

SPECIAL PUBLICATIONS: Information derived from or of value to NASA activities but not necessarily reporting the results of individual NASA-programmed scientific efforts. Publications include conference proceedings, monographs, data compilations, handbooks, sourcebooks, and special bibliographies.

Details on the availability of these publications may be obtained from:

SCIENTIFIC AND TECHNICAL INFORMATION DIVISION

NATIONAL AERONAUTICS AND SPACE ADMINISTRATION

Washington, D.C. 20546